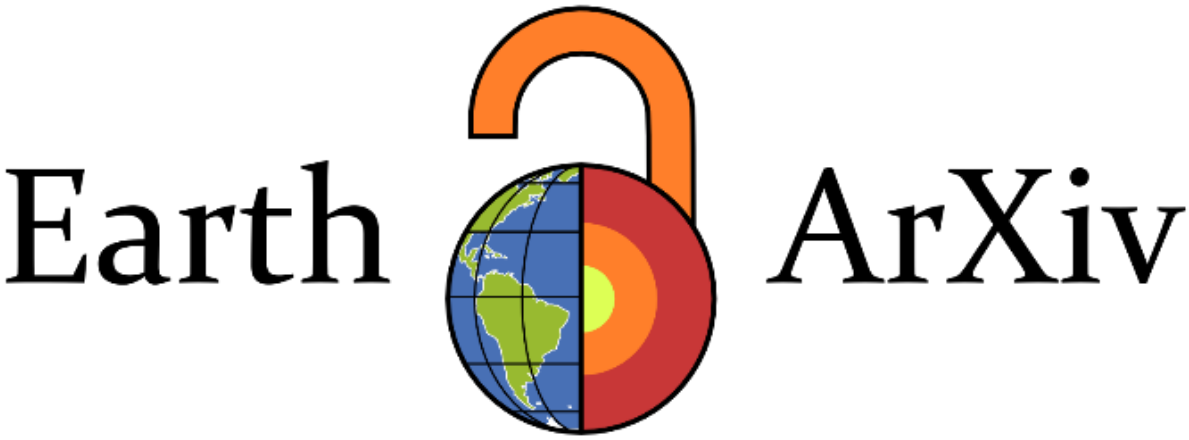

Submitted to GEOPHYSICS on 6 August 2025

A HORIZONTAL VECTOR APPROACH TO 3D ELECTRICAL RESISTIVITY TOMOGRAPHY

Churl Hyun Jo

Subsurface Information Technologies, Inc., Republic of Korea. E-mail: chjo@geeha.co.kr

ABSTRACT

Electrical resistivity tomography (ERT) is commonly implemented with collinear electrode arrays that measure only electric field components along the survey line, neglecting horizontal variations in other directions. This limitation is acceptable in two-dimensional (2D) ERT but can be significant in three-dimensional (3D) settings with complex geometry and strong resistivity contrasts. We propose measuring horizontal vector components of electric field variations, allowing determination of both magnitude and direction of surface electric field changes. Although full inversion tests are not included, incorporating such measurements into inversion frameworks may improve the resolution and reliability of 3D ERT. This concept may provide a new perspective on data acquisition and inversion parameterization.

INTRODUCTION

At present, data acquisition in ERT is typically conducted along linear survey lines with collinear electrode arrays, which measure only the inline component of the electric field. In geological settings with pronounced three-dimensional structures, complex geometry, and strong resistivity contrasts, limiting measurements to the inline component may miss non-negligible information contained in the transverse component**.** Measuring the full horizontal electric-field vector could therefore benefit 3D ERT.

Early attempts were made in the former Soviet Union, where various non-collinear arrays were employed to record both inline and transverse components as documented by Szalai and Szarka(2008). Similar ideas were later pursued by Risk et al. (1970) and Keller et al. (1975) during geothermal exploration, where they measured total electric fields using bipole–dipole arrays and defined corresponding geometric factors. More recently, Szalai et al. (2002) introduced “null arrays” for transverse measurements in dipole–dipole and Schlumberger configurations. These studies illustrate various trials in measuring transverse fields, but none proposed their systematic incorporation into 3D inversion.

Meanwhile, nonlinear iterative inversion algorithms and software frameworks for 3D ERT have advanced considerably (Dey and Morrison, 1979; Loke and Barker, 1996; Yi et al., 1999; Günther et al.,

2006). Yet, to our knowledge, no attempts have been reported to include full horizontal electric-field measurements in inversion datasets.

LIMITATIONS OF CONVENTIONAL ARRAYS

The most widely applied configurations are the Wenner–Schlumberger, dipole–dipole, pole–dipole, and pole–pole arrays, including their variants. Except for the pole–pole array, all are fundamentally collinear. In 2D ERT, collinear arrays are almost exclusively adopted. The measured potential differences then represent only the inline component of the electric field, which is consistent with the 2D assumption of inversion algorithms. In reality, however, subsurface resistivity is inherently three-dimensional, and under complex geometry with strong contrasts, the surface electric field may not develop predominantly along the survey line as commonly assumed. In other words, restricting measurements to the inline component cannot fully represent the surface electric field, ultimately limiting the accuracy of subsurface conductivity estimates.

To demonstrate the need for measuring the full horizontal electric field, we constructed an extreme synthetic model of an arrow-shaped conductor within a resistive host. The model setup and survey geometry are shown in Figure 1a and 1b, and the numerical modeling parameters are summarized in Table 1. A dipole–dipole array was simulated (Figure 1c), with current electrodes marked by squares and potential dipoles deployed for n = 1~10. Four survey lines were tested to examine how the anomaly's position relative to the line influences the response, including transverse measurements comparable to the null array of Szalai et al. (2002).

Figure 2 shows horizontal electric-field vectors plotted along the four survey lines indicated in Figure 1a. In each case, the negative and positive current electrodes were placed at x = 70 m and x = 80 m, respectively. By varying the survey line position (y = 20~50 m), the influence of anomaly proximity and geometry can be clearly seen. The field pattern becomes highly complex, with survey-line crossings near the anomaly edge (Figure 2c) showing the strongest distortions. Because ERT measurements are acquired along survey lines, it is essential to examine how the electric field varies specifically along these lines. Figure 3 summarizes two diagnostic quantities derived from the same lines: (a) the azimuth of the horizontal electric field ($\theta_E = \arctan2(E_y, E_x)$) $\approx \arctan2(-dV_y, -dV_x)$ for dx=dy) and (b) the ratio of the inline component to the total field ($|dV_x|/dV_{\text{total}}$, $dV_{\text{total}} = \sqrt{((dV_x)^2 + (dV_y)^2)}$). Particular attention should be paid to the variation in electric-field orientation in Figure 3a and to the relative contribution of the inline component in Figure 3b. These results demonstrate that the field exhibits significant directional variation, indicating that in certain cases the full horizontal vector needs to be measured rather than relying solely on the inline potential difference.

In practice, the inline component may show negative potential differences along survey lines. For instance, in South Korea, large areas of the basement consist of metamorphosed gneiss with extremely high resistivity. In such settings, when these resistive host rocks are juxtaposed with conductive fault or fracture zones, negative potential differences are often encountered, possibly interpreted to result from

strong resistivity contrasts and complex geometry (Jung et al., 2009). Such field observations motivated this study. Comparable directional distortions are also expected, for example, in landfill investigations with highly conductive contaminants. However, the absence of negative potential measurements in many routine surveys may partly explain why the significance of electric field-direction effects has often been overlooked.

Table 1. Numerical modeling parameters used in the synthetic example.

Parameter	**Value / Description**
Numerical method	3D finite-difference method (FDM)
Solver	Conjugate gradient; relative tolerance = 5×10^{-6}; no preconditioner
Grid size	N_x=121, N_y=49, N_z=49 (with 4 padding layers at all boundaries except surface)
Grid spacing	2.5 m (uniform); padding spacing increases outward by factors of 2, 4, 8, and 16
Host medium resistivity	1000 Ω·m
Overburden (Topsoil)	100 Ω·m, 10 m thick, flat layer
Conductive anomaly	Arrow-shaped, 1 Ω·m, extending from 10 to 50 m depth, 10 m thick

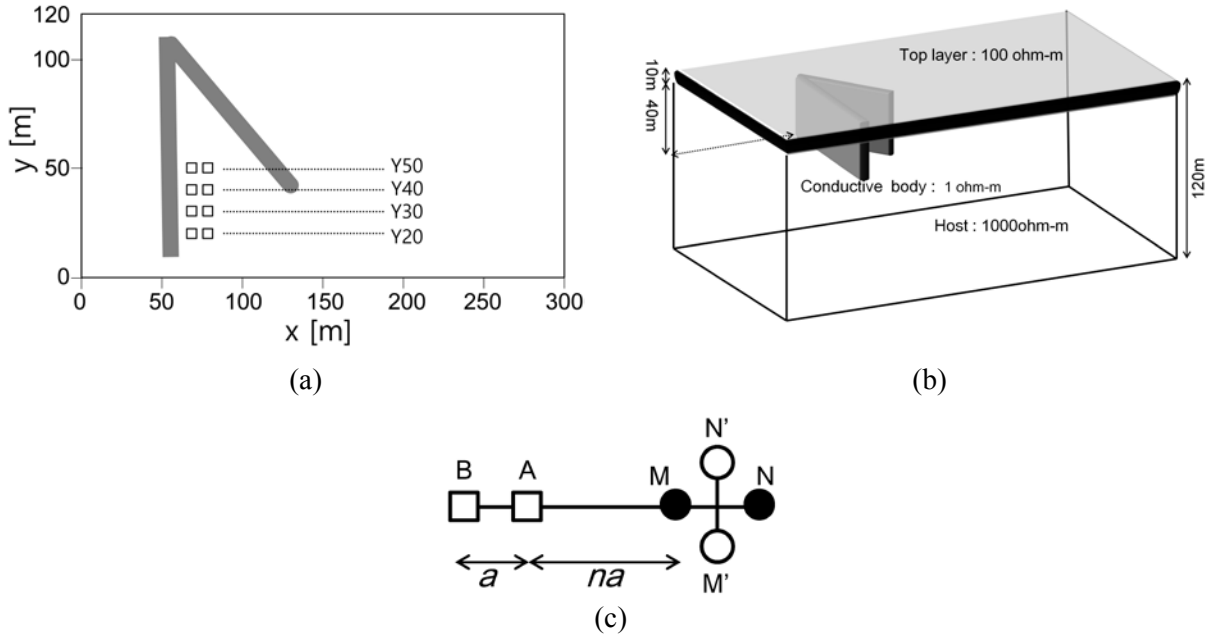

Figure 1. Schematic model and survey configuration for the 3D ERT simulations. (a) Plan view of the conductive anomaly and survey lines(Y20~Y50). The gray arrow-shaped body (1 Ω·m) lies at 10–50 m depth beneath a 10 m thick topsoil layer (100 Ω·m) within a resistive host medium (1000 Ω·m). Dotted lines denote potential electrode coverage, and squares the current electrodes. (b) 3D perspective view of the model. (c) Dipole–dipole array schematic. Current electrodes are denoted A and B; M–N are potential electrodes for inline measurements, and M′–N′ are additional electrodes for transverse measurements. The dipole spacing is *a*, and *n* is the spacing factor.

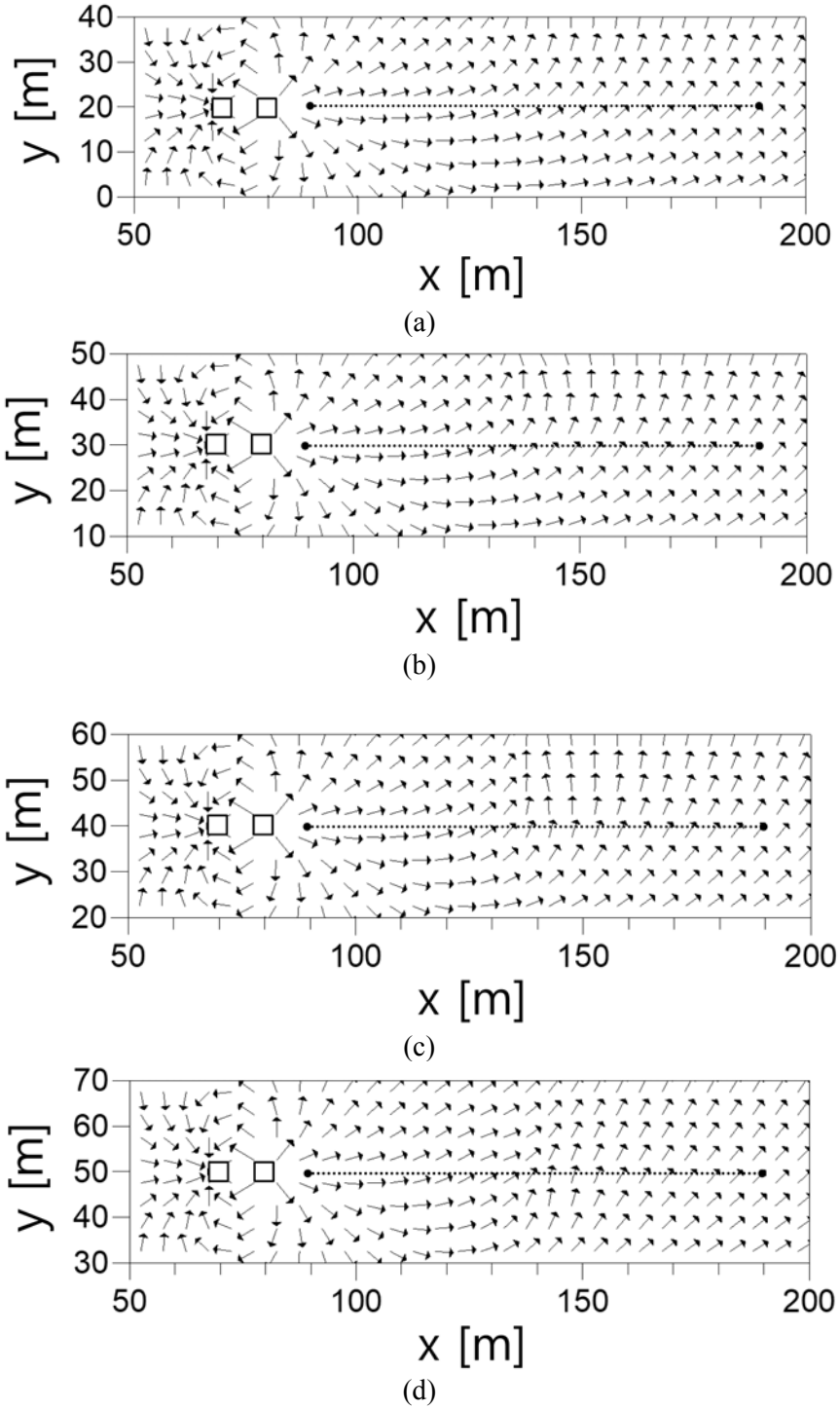

Figure 2. Horizontal electric-field vectors for different current-electrode positions. (a) y = 20 m, (b) y = 30 m, (c) y = 40 m, (d) y = 50 m; current electrodes at x = 70 and 80 m. The current electrodes are shown as open squares, and dotted lines denote the potential electrode coverage (n: 1~10). Vectors are shown at a depth of z = 2.5 m (one grid level below the surface)

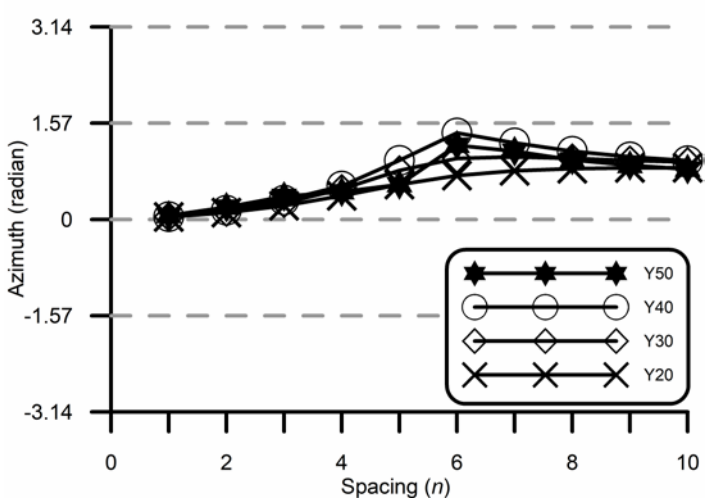

(a)

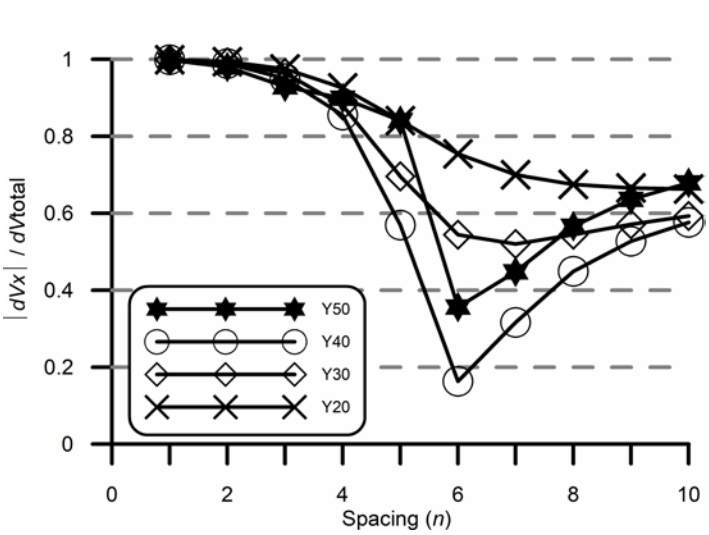

(b)

Figure 3. Calculated horizontal electric field characteristics along survey lines crossing the conductive body (see Figure 1a): (a) azimuth of the horizontal electric field (θ_E = arctan2(E_y, E_x) ≈ arctan2(-dV_y, -dV_x) for dx=dy), (b) ratio of the inline to the total field ($|dV_x|/dV_{total}$).

PROPOSED METHODS

Horizontal Vector Measurements

To overcome the limitations discussed above, we propose a horizontal vector measurement scheme for 3D ERT. As illustrated in Figure 4, two field schemes are considered here. Figure 4a shows the exact implementation of transverse potential electrode pairs perpendicular to the survey line, directly yielding both magnitude and direction of the horizontal field, though at the cost of greatly increased survey effort. Figure 4b illustrates a practical alternative for 3D ERT acquisition in which the survey line spacing equals the electrode station interval. In this scheme, the transverse potential difference can be approximated by pairing M with either Q1 or Q3, or N with either Q2 or Q4. Although these measurements do not correspond exactly to the theoretical ΔV or the precise field angle, they remain meaningful for inversion, provided that the measurement configuration is strictly matched between field acquisition and inversion parameterization.

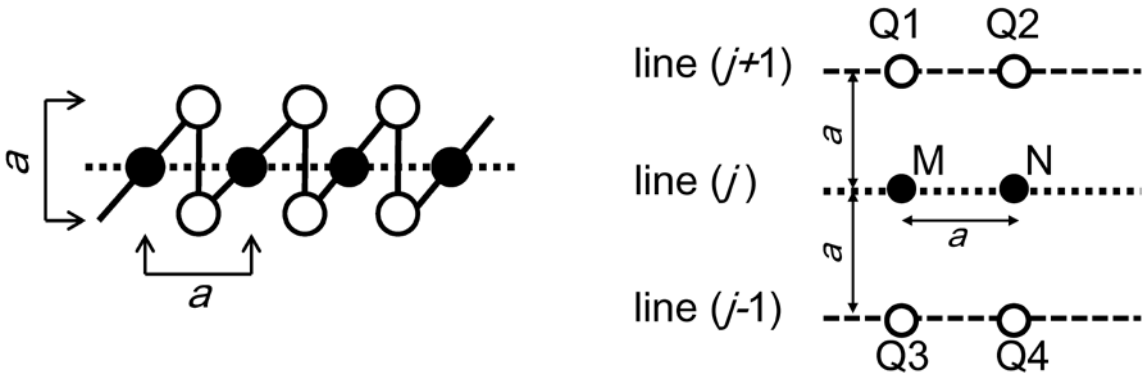

(a) (b)

Figure 4. (a) Exact implementation of the scheme in Fig. 1b. (b) Practical alternative in 3D surveys, where the transverse component is obtained by pairing one electrode on the survey line (dotted line) with another on an adjacent line (dashed lines). Black-filled circles indicate potential electrodes for the inline component, which are also used as current electrodes, and white-filled circles indicate those for the transverse component.

Inversion Parameters

For inversion, we propose extending the conventional single-variable data (inline potential difference) into two complementary parameters: (i) (the logarithm of) the horizontal potential difference magnitude, and (ii) the orientation of the horizontal field vector. This dual-parameter approach can more effectively resolve subsurface resistivity heterogeneity compared to using inline data alone.

CONCLUSION

Generally, data acquisition in 3D ERT surveys is based on the 2D practice of using parallel survey lines with collinear arrays. Yet, when resistivity contrasts are strong, the surface electric field can deviate markedly from the survey-line direction. In such cases, collinear arrays restricted to inline components may provide insufficient information on subsurface resistivity.

This note proposes that 3D ERT be enhanced by including the transverse component of the surface electric field. A horizontal vector measurement scheme enables estimation of both magnitude and orientation of the horizontal field, which can be incorporated as inversion parameters to improve accuracy and reliability. In practice, this requires no modification of existing forward-modeling frameworks—only an extension of inversion parameters—making the approach comparatively straightforward to implement.

The remaining challenge is field acquisition: the proposed scheme requires additional electrodes and longer cabling, while multi-channel instruments to efficiently support it are not yet standard. Nevertheless, these obstacles are likely to be overcome with advances in instrumentation and the ingenuity of field geophysicists.

REFERENCES

Dey, A., and Morrison, H. F., 1979, Resistivity modeling for arbitrarily shaped three-dimensional structures: *GEOPHYSICS*, **44**, no. 4, 753–780.

Günther, T., Rücker C, Spitzer, K., 2006, Three-dimensional modeling and inversion of DC resistivity data incorporating topography—II. Inversion: *Geophysical Journal International*, **166**, Issue 2, 506–517.

Jung, H.-K., Min, D.-J., Lee, H.-S., Oh, S., and Chung, H., 2009, Negative apparent resistivity in dipole-dipole electrical surveys: *Exploration Geophysics*, **40**, 33–40

Keller, G. V., Furgerson, R., Lee, C. Y., Harthil, N., and Jacobson, J. J., 1975, The dipole mapping method: *GEOPHYSICS*, **40**, no. 3, 451–472.

Loke, M.H., and Barker, R. D., 1996, Practical techniques for 3D resistivity surveys and data inversion: *Geophysical Prospecting*, **44**, no. 3, 499–523.

Risk, G. F., Macdonald, W. J. P., and Dawson, C. B., 1970, D.C. resistivity surveys of the Broadlands geothermal region, New Zealand: *Geothermics*, **2**, no. 1, 287–295.

Szalai, S., Szarka, L., Prácser, E., Bosch, F., Muller, I., and Turberg, P., 2002, Geological mapping of near-surface karstic fractures by using null array: *GEOPHYSICS*, **67**, no. 6, 1769–1778.

Szalai, S., and Szarka, L., 2008, On the classification of surface geoelectric arrays: *Geophysical Prospecting*, **56**, no. 2, 159–175.

Yi, M.-J., Kim, J.-H. and Chung, H.-S., 1999, Enhanced resistivity imaging in three dimensions using the least-squares inversion method: *Geophysical Prospecting*, **47**, 843–858.